Food and Chemical Toxicology 156 (2021) 112528

Contents lists available at ScienceDirect

Food and Chemical Toxicology

journal homepage: www.elsevier.com/locate/foodchemtox

Systemic toxicity induced by topical application of heptafluorobutyric acid (PFBA) in a murine model

Lisa M. Weatherly *, Hillary L. Shane, Ewa Lukomska, Rachel Baur, Stacey E. Anderson

Allergy and Clinical Immunology Branch, Health Effects Laboratory Division, National Institute for Occupational Safety and Health, Morgantown, WV, USA

ARTICLE INFO

Handling Editor: Dr. Jose Luis Domingo

Keywords:
PFBA
Heptafluorobutyric acid
Toxicity
Dermal
Liver toxicity

ABSTRACT

Heptafluorobutyric acid (PFBA) is a synthetic chemical belonging to the per- and polyfluoroalkyl substances (PFAS) group that includes over 5000 chemicals incorporated into numerous products. PFBA is a short-chain PFAS (C4) labeled as a safer alternative to legacy PFAS which have been linked to numerous health effects. Despite the high potential for dermal exposure, occupationally and environmentally, dermal exposure studies are lacking. Using a murine model, this study analyzed serum chemistries, histology, immune phenotyping, and gene expression to evaluate the systemic toxicity of sub-chronic dermal PFBA 15-day (15% v/v or 375 mg/kg/dose) or 28-day (3.75–7.5% v/v or 93.8–187.5 mg/kg/dose) exposures. PFBA exposure produced significant increases in liver and kidney weights and altered serum chemistries (all exposure levels). Immune-cell phenotyping identified significant increases in draining lymph node B-cells (15%) and CD11b + cells (3.75–15%) and skin T-cells (3.75–15%) and neutrophils (7.5–15%). Histopathological and gene expression changes were observed in both the liver and skin after dermal PFBA exposure. The findings indicate PFBA induces liver toxicity and alterations of PPAR target genes, suggesting a role of a PPAR pathway. These results demonstrate that sustained dermal exposure to PFBA induces systemic effects and raise concerns of short-chain PFAS being promoted as safer alternatives.

1. Introduction

Per- and polyfluoroalkyl substances (PFAS) are a large group of fluorinated synthetic chemicals used in a wide variety of industrial and consumer processes and products (stain resistant textiles, food packaging material, fire-fighting foams), since the early 1950's because of their physical and chemical properties (Kato et al., 2018; Wang et al., 2017). The vast majority of PFAS are extremely persistent because of the strength of the carbon-fluorine bond. Growing concerns over toxicity associated with PFAS exposure has led to regulatory actions designed to eliminate production of long-chain PFAS, most notably perfluorooctanoic acid (PFOA) and perfluorooctane sulfate (PFOS).

Shorter-chain replacements for these legacy compounds have rapidly emerged and, in general, are promoted as safer alternatives because of the shorter half-lives observed in animal models (Wang et al., 2013). However, recent research suggests exposure to these emerging compounds may result in similar adverse health outcomes as their predecessors (Gomis et al., 2018). Heptafluorobutyric acid (PFBA) is a short-chain PFAS containing 4 carbons with an estimated elimination half-life of hours in mice and several days in humans (ATSDR, 2018), which is much shorter compared to PFOA and PFOS with half-lives of many years in humans (Li et al., 2018). However, several studies show oral exposure of PFBA increases liver weight (Foreman et al., 2009; Das et al., 2008; Butenhoff et al., 2012), similar to that of long-chain PFAS (Biegel et al., 2001; Wolf et al., 2008; Das et al., 2017). Also, in a postmortem evaluation of individuals unknowingly exposed to PFAS via the environment and consumer products, PFBA was detected at similar concentrations to that of PFOA in the liver and higher accumulation was detected in the lungs and kidneys compared to the long-chain PFAS (Pérez et al., 2013). Interestingly, of the 20 PFAS analyzed, PFBA was detected with the highest quantities in both lungs and kidneys (Pérez et al., 2013). Collectively these finding raise concern about the potential toxicity of PFBA.

Much of what we know about PFAS-mediated health effects was generated from epidemiological studies on individuals exposed occupationally, or through accidental releases near chemical manufacturing plants (Heydebreck et al., 2016; Pan et al., 2017; Sun et al., 2016). During 2005–2013, the C8 Science Panel carried out exposure and

* Corresponding author. National Institute for Occupational Safety and Health (NIOSH), 1000 Fredrick Lane, Morgantown, WV, 26505, USA.
E-mail address: nux6@cdc.gov (L.M. Weatherly).

https://doi.org/10.1016/j.fct.2021.112528
Received 15 June 2021; Received in revised form 10 August 2021; Accepted 28 August 2021
Available online 30 August 2021
0278-6915/Published by Elsevier Ltd.

health studies in the Mid-Ohio Valley communities, which had been potentially affected by the releases of PFOA emitted since the 1950s from the Washington Works plant in Parkersburg, West Virginia. Results from these studies suggested associations between long-chain PFAS exposure and certain types of cancers (testicular and kidney), organ toxicity (hepatic, renal, etc.), increased cholesterol levels, decreased thyroid function, alternations in immune function, and reproductive effects (Steenland et al., 2020). Additionally, the National Toxicology Program concluded that both PFOA and PFOS are immune hazards to humans based on evidence from animal and human studies (NTP, 2019). Few epidemiological studies exist on PFBA, however, similar effects are observed with PFBA exposure in animals and include: altered cholesterol levels (Foreman et al., 2009), thyroid function (Butenhoff et al., 2012), reproduction (Butenhoff et al., 2012; Das et al., 2008), and hepatic toxicity (Butenhoff et al., 2012; Foreman et al., 2009).

The potential for dermal exposure to PFAS is high, both during the manufacturing process, as well as in commercial products such as fire-fighting foams and fabric protectants (Begley et al., 2005; Kubwabo et al., 2005). Although there is little exposure information on PFBA specifically, individuals in occupations with contact to PFAS may experience higher exposure, as PFBA is also a breakdown product of other PFAS. Individuals who worked as ski wax technicians showed a significant correlation between years worked and PFBA levels in their blood (Nilsson et al., 2010). In consumer products, PFBA itself has been detected in leather, gloves, carpet, nanosprays, and outdoor textiles (Kotthoff et al., 2015). In the enviornment, PFBA was found at detectable levels in drinking, ground, and surface water (Heo et al., 2014; MDH, 2017; Meng et al., 2019; ATSDR, 2018). As such, there is concern for dermal exposure during bathing or swimming, especially near sites where production once occurred (Wright, 2019). Our lab has previously demonstrated that PFOA is absorbed through the skin (Franko et al., 2012) and dermal PFOA exposure can result in functional immune effects (Shane et al., 2020; Fairley et al., 2007). Despite the potential for dermal exposure, most research has focused on the toxic effects of oral PFBA exposure, and no studies of PFBA dermal exposure were identified. Since the potential for dermal exposure to PFBA is of concern due to both environmental, occupational, and consumer product exposure, it is important to fully understand the potential for dermal penetration and the health risks from exposure to PFBA through the skin.

The present study aims to investigate the systemic effects of subchronic dermal exposure of a short-chain PFAS, PFBA, in a murine model. These findings are important as the short-chain PFAS are being labeled as a safer alternative for the long-chain PFAS and will elucidate the potential health effects of PFBA following skin exposure. Ultimately the collective findings from this study will help to identify and prioritize toxicity while raising awareness about health effects potential.

2. Materials and methods

2.1. Animals

Female $B_6C_3F_1$ mice were used in these studies as they are the National Toxicology Program preferred strain for evaluating general toxicity. All mice were purchased from Taconic (Germantown, NY) at 7–8 weeks of age. Upon arrival, the animals were allowed to acclimate for a minimum of 5 days. All animals were randomly assigned to treatment groups, weighed, and individually identified via tail marking using a permanent marker. Dose groups were identified by cage cards. Both the dosing group as well as the animal numbers were identified on each cage. The animals were housed 5 mice/cage in ventilated plastic shoe box cages with hardwood chip bedding, modified NIH-31 6% irradiated rodent diet (Harlan Teklad – item #7913) and sterile tap water from water bottles *ad libitum*. The temperature in the animal facility was maintained between 65 and 78 °F and the relative humidity between 30 and 70%; a light/dark cycle was maintained at 12-hr intervals. All animal experiments were performed in an AAALAC International accredited National Institute for Occupational Safety and Health (NIOSH) animal facility in accordance with an animal protocol approved by the Institutional Animal Care and Use Committee.

2.2. Test articles and chemicals

Acetone [CAS #67-64-1] and heptafluorobutyric acid (98%; PFBA) [CAS# 375-22-4] were purchased from Sigma-Aldrich. PFBA concentrations were selected based on an initial 7-day range finding study and the highest concentration that did not induce overt toxicity (plus two serial dilutions) were used for these studies.

2.3. PFBA exposures

For all studies, $B_6C_3F_1$ mice (5/group) were topically treated on the dorsal surface of each ear (25 μl/ear) with vehicle or concentrations of PFBA ranging from 3.75 to 15% v/v, once a day for 28 consecutive days at the acetone control, 3.75 and 7.5% exposure doses or intermittently on days 1–8, 14, 15, 17, 18, 22, 25, and 28 for a total of 15 days for the 15% PFBA exposure group due to dermal irritation at the application site. Body weights were measured daily before exposure to ensure no overt toxicity was occurring due to PFBA exposure. Animals were euthanized by CO_2 asphyxiation approximately 24 h after the last exposure.

2.4. Tissue processing

Following euthanasia, animals were weighed, and examined for gross pathology. The liver, spleen, kidneys, and thymus were removed, cleaned of connective tissue, and weighed. Left and right auricular draining lymph nodes (dLNs; draining the site of chemical application) and spleen (1/2) were collected in 4 mL RPMI (Corning). Spleen (1/2) and dLN (2 nodes/animal) cell suspensions were prepared by mechanical disruption of tissues between frosted microscope slides in RPMI and cells were counted after RBC lysis using a Z2 Coulter Particle Count and Size Analyzer (Beckman Coulter). One ear pinna was collected and placed in 4 ml of RPMI for immune phenotyping and half of one ear pinna was placed in 0.5 ml of RNAlater for subsequent gene expression analysis (see below). Ear cell pinna cell suspensions were prepared by splitting the ear pinna into ventral and dorsal halves, followed by an enzymatic digestion for 90 min at 37 °C with 0.25 mg/ml Liberase-TL Research grade (Roche) in RPMI with 100 μg/ml DNase I (Sigma-Aldrich). Digestion was stopped by the addition of 3 ml of RPMI +10% fetal bovine sera (FBS), the ear pinnae + media were transferred to gentleMACS C Tubes (Miltenyi Biotec), and then cells were mechanically disrupted on a gentleMACS™ Dissocciator (Miltenyi Biotec). Following disruption, cells were passed through a 70 μm cell strainer to make a single cell suspension, washed with RPMI +10% FBS, then live cells were counted on a Cellometer using AO/PI (Nexcelom) in order to quantify cells. A small lobe of the liver (caudate) was collected in 0.5 ml of RNAlater for subsequent gene expression (see below). The remainder of the liver, spleen (1/2), ear pinna (1/2), and one kidney (right) was collected in 10% formalin for histopathology analysis.

2.5. Serum chemistries

Blood samples were collected via cardiac puncture, transferred to serum separation tubes, and separated by centrifugation. The serum was frozen at −20 °C for subsequent serum chemistry analysis. Selected serum chemistries were evaluated using a Catalyst DX Chemistry Analyzer (IDEXX Laboratories, Inc.; Westbrook, ME). Endpoints analyzed included: albumin (ALB), globulin (GLOB), alkaline phosphates (ALKP), alanine aminotransferase (ALT), urea nitrogen (BUN), glucose (GLU), total protein (TP), and cholesterol (CHOL).

2.6. Flow cytometry

For staining, single cell suspensions were resuspended in staining buffer containing anti-mouse CD16/32 antibody (Fc Block; BD Biosciences) then incubated with a cocktail of fluorochrome-conjugated antibodies specific for mouse cell surface antigens. For dLN and spleen cells: B220–V500 (RA3-6B2), CD11b-PerCP-Cy5.5 (M1/70), CD8-PE-CF594 (53–6.7), Siglec-F-PE (E50-2440), Ly6G-FITC (1A8) (BD Biosciences), CD11c-eFluor 450 (N418), CD86-APC (GL1) (eBioscience), CD45-Superbright 780 (30-F11), F4/80-PE-Cy7 (BM8), MHCII-APC-eF780 (M5/114.15.2) (Invitrogen), CD4-BV711 (RM4-5), Ly6C-AF700 (HK1.4) (BioLegend). For ear pinna cells: CD4-BV711 (RM4-5), NKp46-BV605 (29A1.4) (BioLegend), CD8-PE-CF594 (53–6.7), CD3-V500 (500A2), Ly6G-FITC (1A8), CD11b-PerCP-Cy5.5 (M1/70), CD11c-AF700 (HL3), Siglec-F-PE (E50-2440) (BD Biosciences), F4/80-PE-Cy7 (BM8), MHCII-APC-eF780 (M5/114.15.2), CD45-Superbright 780 (30-F11), FcεRI-APC (MAR-1) (Invitrogen), CD117-eFluor 450 (2B8) (eBioscience). Cells were then washed, fixed in Cytofix buffer (BD Biosciences), resuspended in staining buffer, and a minimum of 100,000 $CD45^+$ events were collected on a LSR II flow cytometer (BD Biosciences). Compensation controls were prepared with eBioscience UltraComp eBeads. Analysis was performed using FlowJo v10 software (TreeStar Inc., Ashland, OR). All events were gated on single cells using FSC and SSC parameters prior to subsequent gating. Cellular populations were defined using the gating strategies outlined in Supplemental Table 1; Fluorescence minus ones (FMOs) were used as gating controls.

2.7. Gene expression

Ear (half an ear pinna/mouse) and liver (caudate) were homogenized on a TissueLyser II in Buffer RLT (Qiagen). Total RNA was isolated using Qiagen's RNeasy mini spin column kits with DNase treatment on a QIAcube automated RNA isolation machine. RNA concentrations and purity were analyzed on a NanoDrop spectrophotometer (Thermo Fisher Scientific). The cDNA (1–2 μg) was prepared on an Eppendorf Mastercycler using Applied Biosystems' High Capacity Reverse Transcription kit. The cDNA was used on the real-time RT^2 Profiler PCR Array Mouse peroxisome proliferator-activated receptor (PPAR) Targets and Hepatoxicity (QIAGEN; Product #: PAMM-149ZC and PAMM-093ZC) (see Supp. Table 5) and also used as template for real-time PCR reactions containing TaqMan PCR Master Mix with gene-specific primers (Applied Biosystems) on a 7500 Real-Time PCR System. Relative fold gene expression changes ($2^{-\Delta\Delta CT}$) were determined compared to vehicle controls and normalized for expression of reference gene beta-actin (Taqman) or β2-microtubulin (PPAR and Hepatoxicity arrays). Genes that were evaluated are in Supp. Table 2.

2.8. Histology

Tissues were collected in 10% formalin for histopathology. Each tissue sample was embedded in paraffin, sectioned at 5 μm, stained with hematoxylin and eosin (H&E) and evaluated by a veterinary pathologist at StageBio (Mason, Ohio) using The Society of Toxicologic Pathology Guideline (Crissman et al., 2004). Provantis™ pathology software v10.2.3.1 was utilized for data capture and table generation. Histopathology grades were assigned as grade 1 (minimal), grade 2 (mild), grade 3 (moderate), grade 4 (marked), or grade 5 (severe) based on an increasing extent of change. Liver histopathology was a subjective analysis, criteria used for skin grading is shown in Supp. Fig. 3. Representative photographs were taken using a Leica 170HD digital camera mounted on a Leica DM4 B microscope.

2.9. Statistical analysis

A one-way analysis of variance (ANOVA) was conducted for analysis of the data generated from the described animal studies. If the ANOVA showed significance at $p \leq 0.05$, the Dunnett's Multiple Range *t*-test was used to compare treatment groups with the control group. Kruskal-Wallis with Dunn's post-test was conducted for Cd36, Lpl, Serpine1, Pltp, Ehhadh, Krt8, Acox1, Fabp1, Scd1, Il-1β, Il-6, Tslp, S100a7a, S100a8, Cxcl1, and Cxcl2 gene expression analysis due to unequal variance. Statistical analysis was performed using Graph Pad Prism version 5.0 (San Diego, CA). Results represent the mean ± SE of 5 mice per group. Statistical significance is designated by $^*p \leq 0.05$, $^{**}p \leq 0.01$, and $^{***}p \leq 0.001$.

3. Results

3.1. Dermal exposure to PFBA for 28 days results in significant alterations in organ weights

A statistically significant increase in liver and kidney weights (as a % of body weight) was observed following the 28-day exposure to PFBA (Fig. 1A and B). Liver weight significantly increased following exposure to 3.75, 7.5, and 15% PFBA (40%, 65%, and 50%, respectively, vs. values for vehicle-treated mice) (Fig. 1A). Kidney weights were also significantly increased for all three PFBA concentrations (Fig. 1B). No change in weights (as a % of body weight) was observed in the spleen or thymus (Fig. 1C and D). Also, no changes in body weight or overt signs of toxicity were observed following 28-days of PFBA exposure (Supplemental Fig. 1). However, animals exposed to 15% PFBA developed irritation and sensitivity on the ears after ~1 week of exposure. Organ weights not corrected for total body weight are reported in Supplemental Table 3, with significant increases in mass of the kidney (at the 15% PFBA dose) and liver (3.75, 7.5, 15% PFBA doses). No other significant changes in organ weight were observed following exposure to PFBA (Supp. Table 4).

3.2. Dermal exposure to PFBA altered serum chemistries

After 28-days of PFBA exposure there was a significant increase in serum cholesterol, glucose, and alkaline phosphatase (ALKP) and a significant decrease in urea nitrogen (BUN) in the serum (Fig. 2). Cholesterol and ALKP were increased at all three PFBA concentrations with ALKP increasing by 72% with 7.5% PFBA (Fig. 2A, C). Glucose was increased at 3.75 and 15% PFBA (Fig. 1B). BUN was decreased at 15% PFBA (Fig. 2D). No significant changes were observed in alanine aminotransferase, total protein, albumin, or globulin (data not shown).

3.3. Dermal exposure to PFBA for 28 days results in significant phenotypic changes in the skin and dLN

Overall, there was no change in total cellularity after 28 days of exposure to PFBA in the dLN (Table 1). However, in the dLN significant decreases were observed in the frequency of both CD4 and CD8 T-cells at 7.5% and 15% PFBA (Table 1). A significant increase in the absolute number of dendritic cells (DCs) (7.5% and 15%) and an increase in both frequency and cell number in B-cells (15%) and CD11b + cells (3.75%, 7.5%, 15%) was also observed. The median fluorescent intensity (MFI) of MHCII on B-cells was also significantly increased at all three PFBA concentrations (Table 1).

Phenotypic analysis of the ear pinna following 28 days of PFBA exposure resulted in increases in frequency of $CD45^+$ cells (7.5%, 15%), CD4 T-cells (3.75%, 7.5%, 15%), CD8 T-cells (3.75%, 7.5%), NK cells (7.5%, 15%), eosinophils (3.75%, 7.5%, 15%), neutrophils (7.5%, 15%), and CD11b + DCs (15%) (Table 2). Statistically significant increases were also observed in the absolute number of total cells, $CD45^+$ cells, CD4 and CD8 T-cells, NK cells, eosinophils, neutrophils, CD11b- DCs, and CD11b + DCs.

Fewer changes were observed in the spleen showing a significant decrease in the absolute number of total cells (7.5%), B-cells (7.5%), CD4 T-cells (7.5%), neutrophils (7.5%), and CD11b + cells (7.5%)

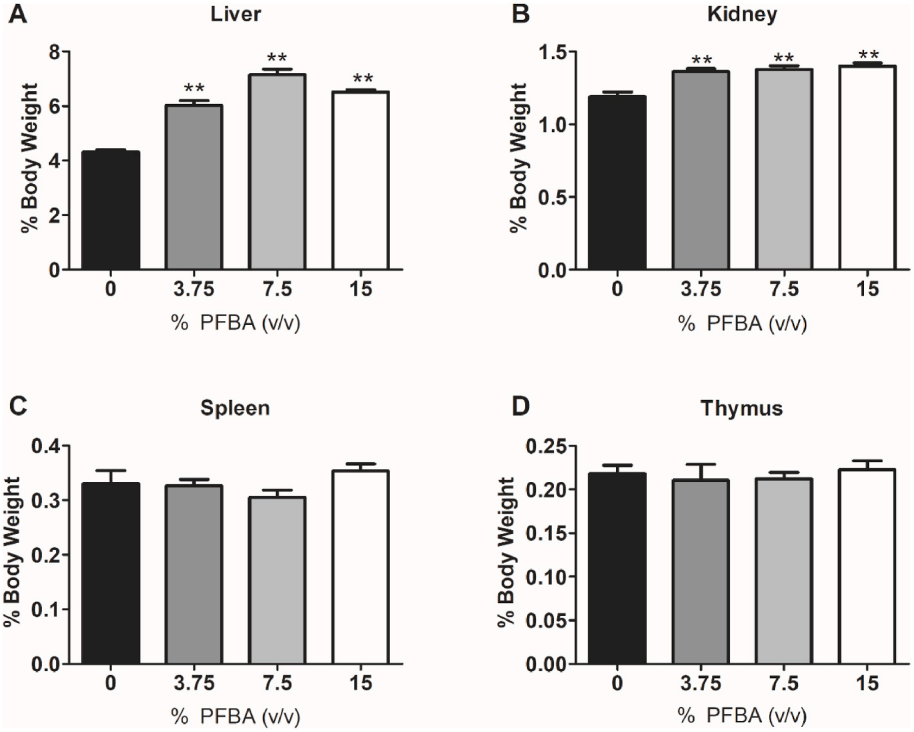

Fig. 1. Changes in organ weights after dermal exposure to PFBA. Analysis of changes in liver (A), kidney (B), spleen (C), and thymus (D) weights following 28 days of PFBA exposure. Data is displayed as organ weight as % of body weight. Each concentration represents mean (±SE) of 5 mice per group. Statistical significance, relative to 0% vehicle control, was determined by one-way ANOVA followed by Dunnett's post-test indicated as **p < 0.01. Note: The 15% PFBA exposure group received treatment on days 1–8, 14, 15, 17, 18, 22, 25, and 28 for a total of 15 days.

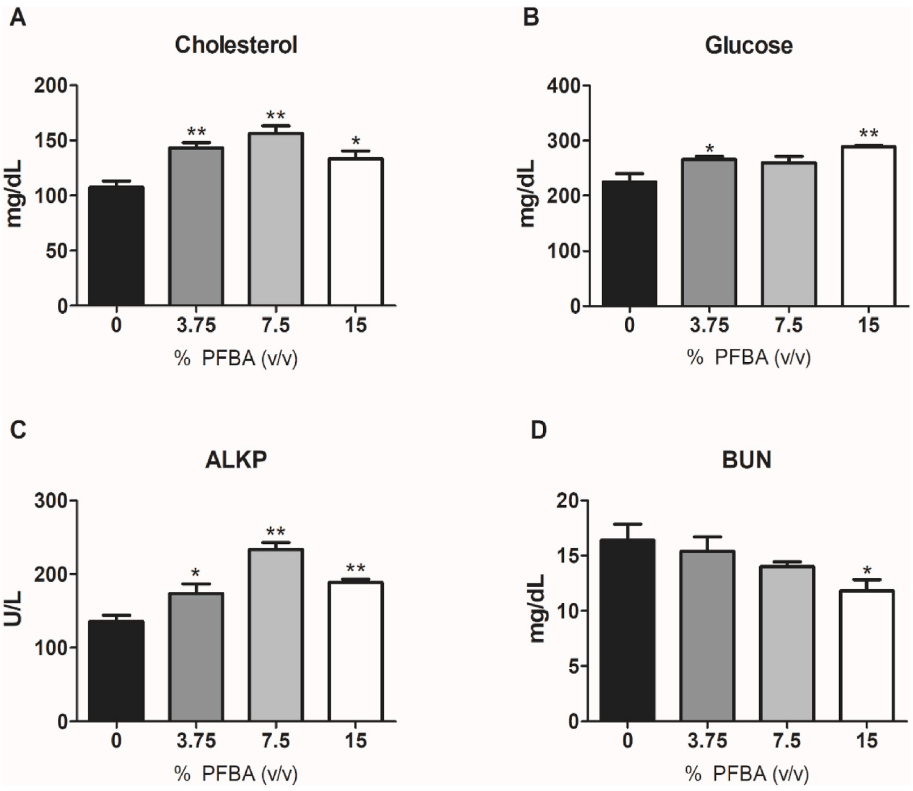

Fig. 2. Changes in serum chemistry after dermal exposure to PFBA. Analysis of changes in cholesterol (A), glucose (B), ALKP (C), and BUN (D) following 28 days of PFBA exposure. Each concentration represents mean (±SE) of 5 mice per group. Statistical significance, relative to 0% vehicle control, was determined by one-way ANOVA followed by Dunnett's post-test indicated as *p < 0.05, **p < 0.01. Note: The 15% PFBA exposure group received treatment on days 1–8, 14, 15, 17, 18, 22, 25, and 28 for a total of 15 days.

(Supp. Table 5). An increase in MFI of MHCII was observed on B-cells and DCs and of CD86 on B-cells and DCs.

3.4. Dermal exposure to PFBA for 28 days results in histopathological changes in the liver and skin

In the liver, histopathological examination revealed that PFBA induced hepatocellular hypertrophy in all animals with all three PFBA exposures, with the greatest severity being observed at the 7.5%

Table 1
Draining lymph node phenotyping of mice dermally exposed to PFBA.

dLN	28 days			
Parameter	0%	3.75%	7.5%	15%
Cellularity (x 10^7)	1.0 ± 0.2	1.0 ± 0.2	1.3 ± 0.04	1.4 ± 0.03
$CD4^+$ (x 10^6)	4.3 ± 0.7	4.4 ± 0.6	4.8 ± 0.1	4.5 ± 0.1
$CD4^+$ (%)	42.3 ± 0.6	43.4 ± 1.2	37.8 ± 0.5**	32.1 ± 0.8***
$CD8^+$ (x 10^6)	3.0 ± 0.5	3.2 ± 0.5	3.4 ± 0.5	3.1 ± 0.1
$CD8^+$ (%)	30.0 ± 0.7	31.9 ± 0.9	26.8 ± 0.4*	22.0 ± 0.4***
B-cells (x 10^6)	2.0 ± 0.4	1.5 ± 0.3	2.7 ± 0.1	4.4 ± 0.2***
B-cells (%)	19.0 ± 0.9	13.9 ± 1.2**	21.5 ± 0.3	31.2 ± 1.1***
NK (x 10^4)	5.6 ± 0.7	6.7 ± 0.9	7.8 ± 0.3	10.2 ± 0.1***
NK (%)	0.6 ± 0.1	0.6 ± 0.1	0.6 ± 0.1	0.7 ± 0.1
DCs (x 10^4)	8.7 ± 2.3	11.6 ± 1.2	16.9 ± 0.1**	15.3 ± 1.4*
DCs (%)	0.8 ± 0.2	1.2 ± 0.1	1.3 ± 0.1	1.1 ± 0.1
CD11b+ (x 10^5)	1.6 ± 0.4	2.4 ± 0.4	4.2 ± 0.3***	6.3 ± 0.4***
CD11b+ (%)	1.5 ± 0.1	2.3 ± 0.2*	3.3 ± 0.2***	4.5 ± 0.3***
MHCII B-cells (MFI)	2874.6 ± 163.8	3725.2 ± 361.0*	4805.0 ± 114.1***	4632.8 ± 191.6***
MHCII DCs (MFI)	19826.0 ± 1995.5	19727.8 ± 1344.9	16387.0 ± 314.6	15132.0 ± 280.1*
CD86 B-cells (MFI)	502.6 ± 19.4	491.6 ± 36.8	537.4 ± 17.9	483.8 ± 18.5
CD86 DCs (MFI)	2316.6 ± 197.5	2612.8 ± 157.3	2087.8 ± 36.1	2305.0 ± 86.4

Values are expressed as the means (±SE) for each group (n = 5 mice/group). *p < 0.05, **p < 0.01, ***p < 0.001.

Table 2
Skin phenotyping of mice dermally exposed to PFBA.

Skin	28 days			
Parameter	0%	3.75%	7.5%	15%
Cellularity (x 10^5)	8.6 ± 0.9	9.1 ± 0.6	16.6 ± 0.8***	12.0 ± 2.0
$CD45^+$ (x 10^4)	5.2 ± 0.8	6.1 ± 0.6	25.3 ± 0.3**	21.6 ± 0.6**
$CD45^+$ (%)	5.9 ± 0.4	6.7 ± 0.3	15.1 ± 1.5**	16.7 ± 2.7***
$CD4^+$ (x 10^3)	1.3 ± 0.3	2.3 ± 0.2	12.7 ± 1.1***	8.3 ± 2.0**
$CD4^+$ (%)	2.3 ± 0.2	3.8 ± 0.2**	5.1 ± 0.2***	4.1 ± 0.3***
$CD8^+$	34.4 ± 4.1	129.2 ± 27.7	727.0 ± 59.2***	338.4 ± 64.1***
$CD8^+$ (%)	0.07 ± 0.005	0.22 ± 0.05*	0.30 ± 0.04***	0.18 ± 0.02
NK (x 10^2)	3.9 ± 0.5	4.0 ± 0.3	29.3 ± 4.5***	19.2 ± 4.9*
NK (%)	0.77 ± 0.02	0.66 ± 0.05	1.14 ± 0.05***	0.92 ± 0.04*
Eosinophils (x 10^3)	1.6 ± 0.4	3.5 ± 0.5	21.6 ± 3.1***	14.9 ± 4.4**
Eosinophils (%)	2.9 ± 0.3	5.7 ± 0.4**	8.6 ± 0.7***	6.5 ± 0.7***
Neutrophils (x 10^2)	0.9 ± 0.2	2.7 ± 0.6	117.0 ± 36.4	216 ± 58.0**
Neutrophils (%)	0.16 ± 0.02	0.42 ± 0.07	4.4 ± 1.1***	10.2 ± 0.4***
CD11b- DCs (x 10^2)	3.8 ± 0.9	5.4 ± 0.6	13.9 ± 1.3***	5.4 ± 1.2
CD11b- DCs (%)	0.69 ± 0.07	0.87 ± 0.04	0.57 ± 0.06	0.27 ± 0.03***
CD11b + DCs (x 10^2)	1.2 ± 0.6	2.5 ± 0.3	7.9 ± 1.4	13.5 ± 3.6**
CD11b + DCs (%)	0.20 ± 0.07	0.41 ± 0.04	0.33 ± 0.07	0.63 ± 0.04***

Values are expressed as the means (±SE) for each group (n = 5 mice/group). *p < 0.05, **p < 0.01, ***p < 0.001.

exposure (Table 3). Hepatocellular hypertrophy was characterized by increased cytoplasmic eosinophilia, decreased glycogen content, and increased cellular volume of hepatocytes in centrilobular locations.

Table 3
Incidence and degree of hepatocyte injury following dermal exposure to PFBA in mice.

Liver	28 days			
Parameter	0%	3.75%	7.5%	15%
Hypertrophy, centrilobular, hepatocyte				
Minimal	0	3	0	0
Mild	0	2	2	5
Moderate	0	0	3	0
Necrosis, subcapsular, hepatocyte				
Minimal	0	1	0	0
Moderate	0	0	1	0

Individual animals treated with 3.75% PFBA showed mild centrilobular hepatocyte hypertrophy (2/5 mice) and 1/5 mice showed minimal hepatic focal necrosis (Table 3). With 7.5% PFBA 1/5 mice exhibited moderate multifocal subcapsular necrosis of hepatocytes and 3/5 mice showed moderate hypertrophy (Fig. 3B and C; Table 3). At 15% PFBA mild hypertrophy was seen in all 5 mice (Table 3). No histopathological changes were observed in the liver with 0% PFBA vehicle control.

In the skin, dose-related epidermal, dermal, and cartilaginous changes were observed (Table 4). Epidermal hyperplasia was characterized by increased number of keratinocyte layers with increased hyaline granules in the more severely affected areas. Hyperkeratosis occurred in areas of epidermal hyperplasia and was characterized by increased amounts of compacted keratin that was either artifactually detached from the surface or tightly adhered to the surface of the epidermis. At 3.75% PFBA, 5/5 mice exhibited minimal hyperplasia (3–4 layers of keratinocytes) and minimal hyperkeratosis (Fig. 4B; Table 4). Erosions/ulcers were characterized by partial or full thickness defects in the epidermis that were associated with neutrophilic inflammation. Fibrosis was characterized by increased amounts of collagenous stroma with scattered fibroblasts that expand the dermal thickness beneath the hyperplastic epidermis. At 7.5% PFBA, 4/5 mice showed mild focal epidermal hyperplasia (5–6 layers of keratinocytes) with mild ulceration/erosion (1/5 mice), moderate hyperkeratosis (2/5 mice), and mild fibrosis (3/5 mice) (Fig. 4C; Table 4). Necrosis of the epidermis was characterized by superficial or full thickness loss of differential staining with retention of cellular detail (coagulative necrosis) without inflammation. At 15% PFBA, 3/5 mice showed moderate dermal fibrosis, moderate multifocal epidermal necrosis (3/5 mice) (Fig. 4D; Table 4), moderate epidermal hyperplasia (3/5 mice), and moderate epidermal hyperkeratosis (4/5 mice) (Fig. 4E; Table 4). All animals at 7.5% and 15% showed mixed cell inflammation. This was characterized by neutrophils, lymphocytes, and/or macrophages scattered within the fibrosis and sometimes in areas of ulceration or erosion, when present (Table 4). No histopathological changes were observed in the skin with 0% PFBA vehicle control. No histopathological changes were observed in the spleen or kidney (data not shown).

3.5. Dermal PFBA exposure results in changes in liver and skin gene expression

To examine the mechanisms driving the systemic toxicity following PFBA exposure, two PCR pathway-based arrays were conducted with liver mRNA. PPAR targets and hepatoxicity arrays showed significant increases in multiple genes (Supp. Table 6). Genes involved in cholestasis (*Abcd4, Abcc2, Abcc3*), steatosis (*Cd36, Fasn, Lpl, Scd1*), phospholipidosis (*Fabp1, Hpn, Lss*), hepatoxicity (*Aldoa, Apex1, Btg2, Ccng1, Gadd45a, Gclc, Gsr, Krt18, Krt8, Nqo1*), nongenotoxic hepatocarcinogenicity (*Aldoa, Apex1, Btg2, Ccng1, Krt8, Krt18*), necrosis (*Col4a1, Ipo4, Osmr, Serpine1*), adipogenesis (*Lpl*), fatty acid metabolism (*Pltp, Scd1*), lipid transport (*Lpl*), and PPAR ligand transport (*Cd36, Fabp5*) were upregulated (Supp. Table 6). The transcripts with the highest fold increase were chosen to be confirmed via TaqMan qPCR. Increases in *Cd36* was observed at 3.75% (17-fold) and *Lpl* at 3.75% and

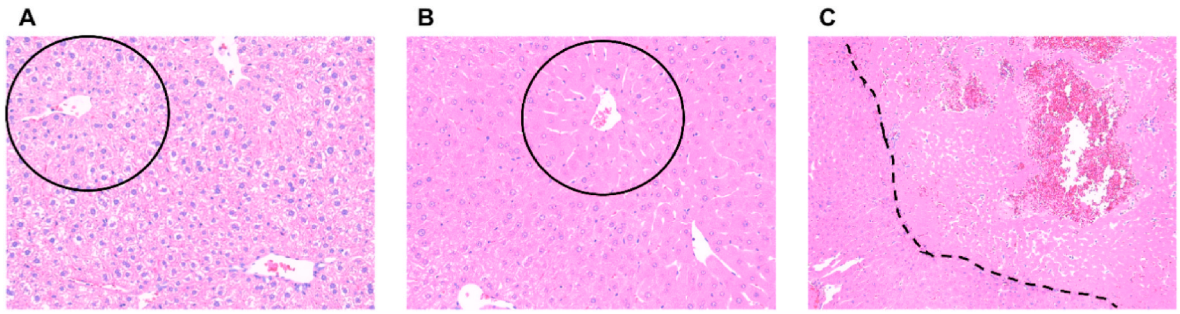

Fig. 3. Histopathology of liver following dermal exposure to PFBA. Representative H&E-stained liver sections from control and 7.5% PFBA-treated mice. Vehicle control 0% PFBA exposure shows normal liver with regular sized centrilobular hepatocytes and normal cytoplasmic rarefaction (black circle), 20X magnification (A). Moderate centrilobular hepatocyte hypertrophy (black circle) was found in 7.5% PFBA exposed mice, 20X magnification (B). Also, at 7.5% PFBA, moderate multifocal hepatocyte necrosis (right of dotted line) was found, 10X magnification (C). Note: The 15% PFBA exposure group received treatment on days 1–8, 14, 15, 17, 18, 22, 25, and 28 for a total of 15 days.

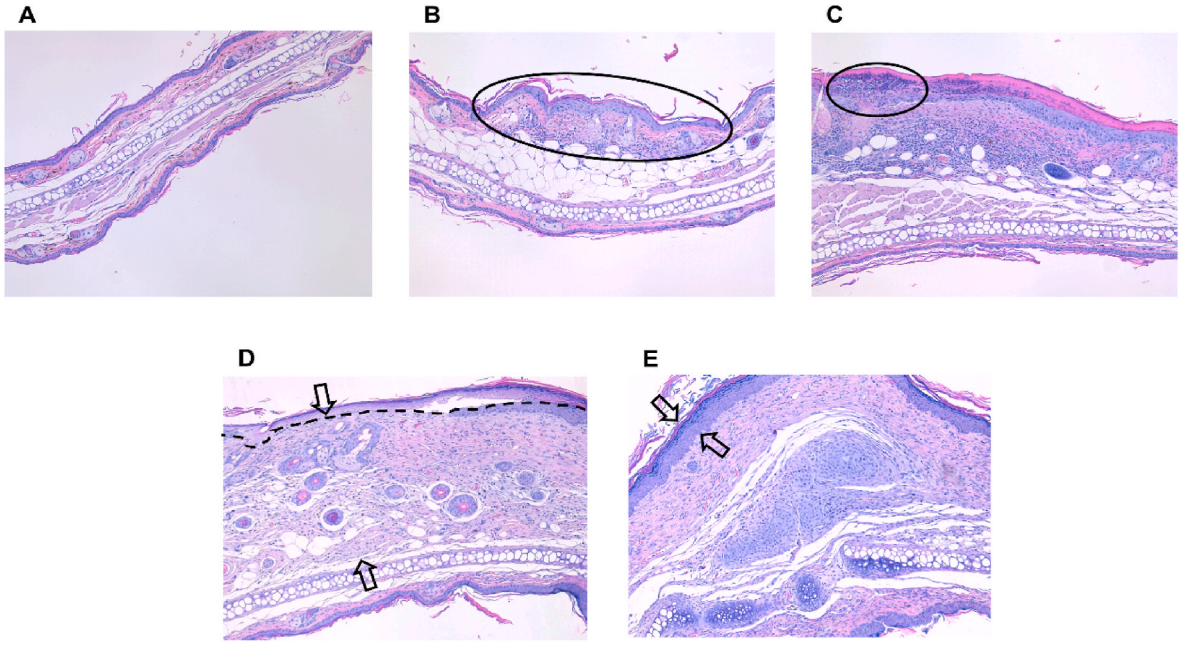

Fig. 4. Histopathology of skin following dermal exposure to PFBA. Representative H&E-stained ear pinna sections from control and PFBA-treated mice. Vehicle control 0% PFBA exposure (A). Minimal focal epidermal hyperplasia with minimal hyperkeratosis and mixed cell inflammation (oval) was found at 3.75% PFBA (B). Mild focal epidermal hyperplasia with mild ulceration/erosion (oval), moderate hyperkeratosis, mild fibrosis, and mild mixed cell inflammation was found at 7.5% PFBA (C). At 15% PFBA, moderate dermal fibrosis (between arrows), with moderate multifocal epidermal necrosis (above dotted line) (D) and moderate epidermal hyperplasia (between arrows) with moderate epidermal hyperkeratosis (E) was found. All images are 10X magnification. Note: The 15% PFBA exposure group received treatment on days 1–8, 14, 15, 17, 18, 22, 25, and 28 for a total of 15 days.

7.5% (44-fold) PFBA (Fig. 5A and B). Gene expression of *Serpine1* increased at 7.5% (11-fold) and 15% (12-fold) and both *Pltp* and *Ehhadh* (involved in fatty acid metabolism) increased at two PFBA concentrations with *Ehhadh* increased 73-fold at 7.5% PFBA (Fig. 5C, D, E). An increase in *Krt8* and *Scd1* was only demonstrated at 7.5% PFBA (3.3 and 2.5-fold, respectively) (Fig. 5F, I). *Acox1* significantly increased at 7.5% (7.7-fold) and 15% (9.1-fold) and *Fabp1* increased at 15% (5.1-fold) (Fig. 5G and H). No significant changes were observed in *Fabp5*, *Ppara*, or *Nfκb* (Fig. 5J-L).

To help better define the mechanism of dermal toxicity, select genes were evaluated in the skin following PFBA exposure. Inflammatory cytokines *Il-1β* and *Il-6*, although not significantly increased via ANOVA, have a significant linear trend increase (Linear Trend Test $p < 0.05$) and with 15% PFBA have a 22-fold and 6-fold increase, respectively (Fig. 6A and B). The Th2 skewing cytokine, *Tslp*, increased with 7.5% and 15% (12-fold) PFBA exposure (Fig. 6C). Expression of both danger-associated molecular patterns (DAMPs) *S100a7a* and *S1008a* increased, with *S100a7a* increasing at 3.75% PFBA (6-fold) and *S100a8* increasing at 7.5% and 15% (18-fold) (Fig. 6E and F). *Serpine1*, involved in necrosis, increased at 7.5% (3-fold) and 15% (4-fold) PFBA exposure (Fig. 6I). Interestingly, *PPARα* decreased at both 7.5% and 15% PFBA (Fig. 6D). The chemokines *Cxcl1* and *Cxcl2* have a significant linear trend increase (Linear Trend Test $p < 0.05$), with *Cxcl2* having a 52-fold increase at 7.5% PFBA (Fig. 6G and H). No changes were observed in any of the 6 skin barrier integrity genes (*Flg2, Itgbl1, Lor, Flg, Krt10, Krt14*) examined (Supp. Fig. 2).

4. Discussion

The skin is a portal for entry of toxic substances into the body and The Centers for Disease Control and Prevention (CDC) estimates that more than 13 million workers in the United States, spanning a variety of occupational industries and sectors, are potentially exposed to chemicals that can be absorbed through the skin (NORA, 2019). Approximately 82,

Table 4
Incidence and degree of epidermal and dermal injury following dermal exposure to PFBA in mice.

Skin (ear)	28 days			
Parameter	0%	3.75%	7.5%	15%
Hyperplasia, epidermis, focal				
Minimal	0	5	1	1
Mild	0	0	4	1
Moderate	0	0	0	3
Hyperkeratosis, epidermis, focal				
Minimal	0	4	2	0
Mild	0	0	1	1
Moderate	0	0	2	4
Necrosis, epidermis, multifocal				
Minimal	0	0	2	0
Mild	0	0	2	1
Moderate	0	0	0	3
Marked	0	0	0	1
Inflammation, mixed cell, dermis				
Minimal	0	1	2	3
Mild	0	0	3	2
Erosion/ulcer, focal or multifocal				
Minimal	0	0	2	2
Mild	0	0	1	0
Fibrosis, dermis, focal				
Minimal	0	0	1	0
Mild	0	0	3	2
Moderate	0	0	0	3

000 chemicals are in industrial use with an estimated additional 700 new chemicals being introduced annually (Tollefson, 2016) resulting in a high potential for dermal exposure to chemicals. Occupational skin exposures can result in numerous diseases which can adversely affect an individual's health and capacity to perform at work resulting in significant economic losses (Cashman et al., 2012; Mancini et al., 2008). Therefore, it is critical to understand how skin exposures of chemicals contribute to systemic toxicity.

Toxicity related to PFAS exposure is of growing concern both occupationally and for the public, however, investigations into the systemic effects related to dermal exposure are lacking. To the best of our knowledge, these are the first studies to evaluate systemic toxicity following sub-chronic dermal exposure to PFBA in a murine model. Alterations in organ weights, organ histology, and serum chemistries support that PFBA can be absorbed through the skin. Similar to PFOA, the systemic effects of PFBA that occurred after dermal exposure were identified mainly in the liver, which plays a major role in the metabolism of chemicals. Both hepatomegaly (Fig. 1A) and hepatocellular hypertrophy (Fig. 3; Table 1) were observed after dermal exposure to all three PFBA concentrations. Previous studies on the legacy long-chain PFAS, PFOA and PFOS, demonstrated hepatocellular hypertrophy and alterations in lipid metabolism (Kennedy et al., 2004; Lau et al., 2007). In this study, dermal PFBA exposure increased liver weights (as a % of body weight) in a similar manner to that of PFOA exposure (Das et al., 2017; Shane et al., 2020), although the increase was to a lesser extent despite higher concentrations of PFBA exposure. Additionally, multiple studies have observed similar changes in liver weights and hepatocellular hypertrophy in both rats and mice and in males and females at multiple oral PFBA doses (Butenhoff et al., 2012; Das et al., 2008; Permadi et al., 1992, 1993). Oral exposure for 28 days increased liver weight in rats by 45% with 150 mg/kg/day NH_4^+PFBA (Butenhoff et al., 2012) and oral exposure for 17 days increased relative liver weight by ~40% with 175 mg/kg/day NH_4^+PFBA in pregnant mice (Das et al., 2008), compared to the current 28-day dermal exposure of 7.5% PFBA (~187.5 mg/kg/day) increasing liver weight by 63% (compared to control). It is important to note that NH_4^+PFBA salt has ~8% difference in molar concentration from the free acid dose. An enlarged liver can be caused by steatosis, an accumulation of fat in the liver due to metabolic dysfunction. Liver lipoprotein lipase (LPL) and fatty acid translocase (CD36) are involved in steatosis where LPL helps control lipid intake and CD36 plays a key role in transporting lipids to the liver from the blood. Gene expression of *Cd36* and *Lpl* were two of the most upregulated genes in PFBA-exposed liver (Fig. 5; Supp. Fig. 4). Genes involved in fatty acid metabolism (*Acox1, Ehhadh, Pltp, Scd1*) were also greatly upregulated (Fig. 5; Supp. Fig. 4). The increase in these transcripts following dermal PFBA exposure are consistent with earlier studies of PFOA exposure that showed an increase in the same transcripts (*Cd36, Acox1, Scd1, Lpl*) in the livers of mice (Das et al., 2017; Yan et al., 2015; Hui et al., 2017). Further support for liver dysfunction was demonstrated by significant changes in serum ALKP, BUN, cholesterol, and glucose (Fig. 2). A fatty liver can lead to an increase in glucose and cholesterol while serum cholesterol can be elevated in cholestasis; we observed an increase in multiple genes associated with cholestasis (*Abcd4, Abcc2, Abcc3*) (Supp. Fig. 5). PFOA exposure has been shown to also lead to an increase in glucose and cholesterol in both animal (Du et al., 2018; Zheng et al., 2017; Rebholz et al., 2016) and epidemiology studies (Liu et al., 2018). These data indicate that dermal PFBA exposure has similar effects on the liver compared to oral PFBA and PFOA exposure.

PPARα plays a role in metabolic functions, energy homeostasis, and inflammation. Studies with the long-chain PFAS, PFOA, suggest that PPARα activation is the key factor in PFOA-induced toxicity and liver dysfunction (Kennedy et al., 2004; Lau et al., 2007). Although data is conflicting, a PPARα-dependent pathway has been suggested for oral PFBA-induced liver dysfunction (Foreman et al., 2009). In the current study, *PPARα* itself was only slightly upregulated in the liver microarray (Supp. Table 6) and no significant increases were observed in *PPARα* qPCR (Fig. 5K). However, multiple genes that are PPAR targets (Rakhshandehroo et al., 2010) were upregulated in the liver (Fig. 5). It is possible that PPAR isoforms other than *PPARα* are responsible for the increases in transcripts, as *PPARγ* and *PPARβ/δ* can be found in the liver and have overlapping functions with *PPARα* (DeLuca et al., 2000; Zhang et al., 2006; Rogue et al., 2010).

However, PPARα-independent pathways have also been suggested. Evidence of hepatic effects resulting from PPARα-independent pathways from long-chain PFAS, including PFOA and PFOS, demonstrate activation of pregnane X receptor (PXR), constitutive active receptor (CAR), along with additional PPAR isoforms PPARγ and PPARβ/δ (Abe et al., 2017; Das et al., 2017; Zhang et al., 2017; Rosen et al., 2017; Vanden Heuvel et al., 2006; Bjork et al., 2011; Takacs and Abbott, 2007). Using PPAR knock-out mice, PFOA induced enlarged livers (Abbott et al., 2007; Wolf et al., 2008) and altered the expression of genes involved in fatty acid metabolism and inflammation (Rosen et al., 2008) also supporting the involvement of a PPARα-independent pathway.

In order to further investigate the mechanism of toxicity following dermal PFBA exposure, *PPARα* expression was also examined in the skin. After a 28-day exposure, PFBA did not increase *PPARα* in the skin but rather induced a significant decrease at both 7.5% and 15% (Fig. 6D). This is similar to the decrease in *PPARα* expression observed after PFOA dermal exposure (Shane et al., 2020). While the biological significance is unknown, the observed *PPARα* results in the skin suggest PFBA might be activating a nuclear receptor other than PPARα or that PFBA induces increases in *PPARα* at an earlier time point. Dermal PFOA exposure exhibited a decrease in skin barrier genes after 4 and/or 14 days of exposure (Shane et al., 2020), therefore these were examined in the present study. However, no change was observed in any skin barrier genes investigated in this study (Supp. Fig. 2). This result could be due to timing as the skin barrier genes were only measured after a 28-day exposure.

As PPARα is considered to exert anti-inflammatory effects, consistent with a decrease in *PPARα*, there are also persistent signs of inflammation evidenced by an increasing trend in *Il-6* and *I-lβ* in the skin (Fig. 6A and B). Additionally, other studies have shown PPARα knock-out mice produced significantly more IL-6 (Poynter and Daynes, 1998). Also, in support of a sustained inflammatory response is an increase in the number and frequency of macrophages and number of neutrophils in the dLN (Table 1), and an increase in the number and frequency of T-cells,

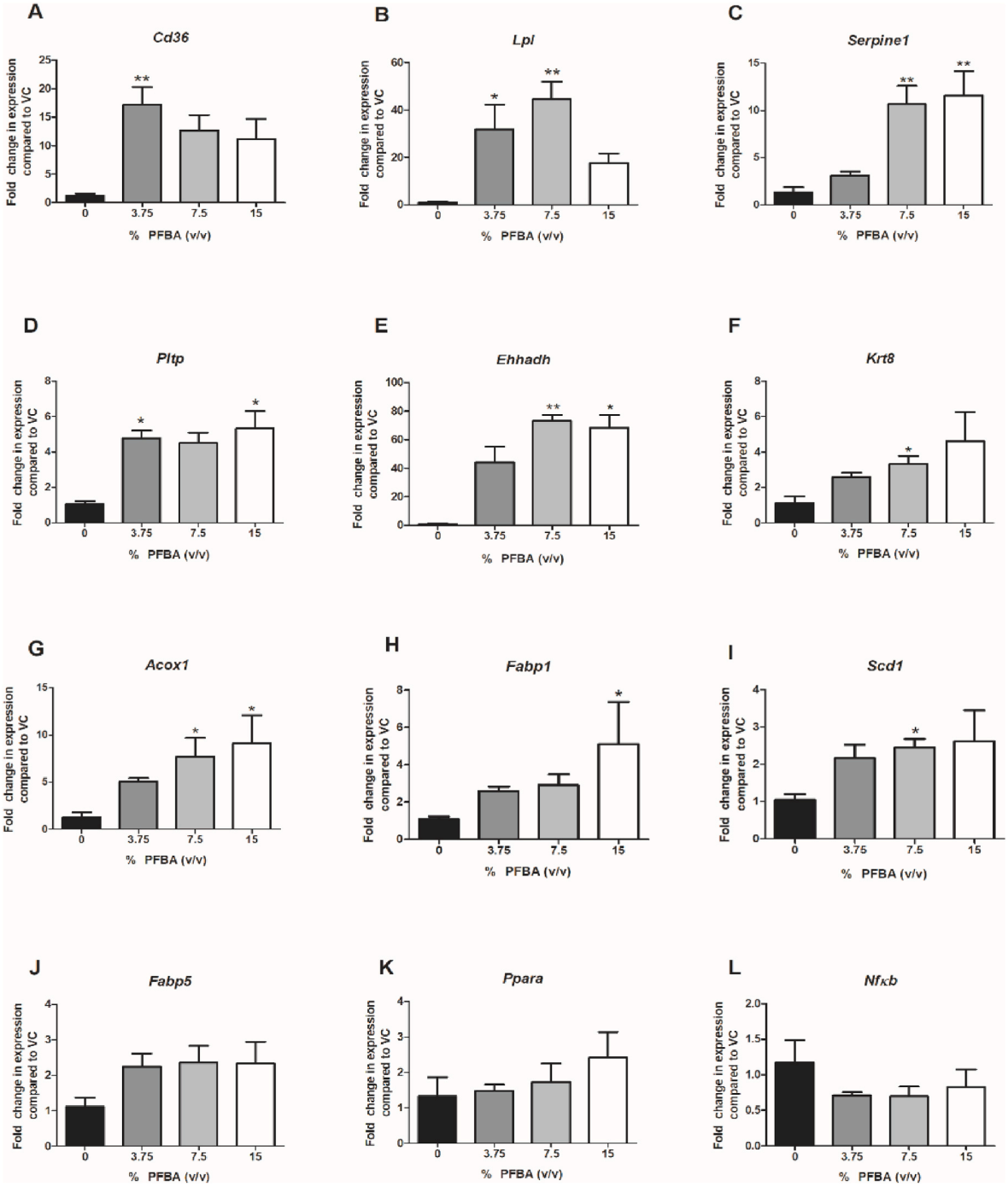

Fig. 5. Liver gene expression following dermal exposure to PFBA. Gene expression in the liver following 28 days of PFBA exposure. Changes in *Cd36* (A), *Lpl* (B), *Serpine1* (C), *Pltp* (D), *Ehhadh* (E), *Krt8* (F), *Acox1* (G), *Fabp1* (H), *Scd1* (I), *Fabp5* (J), *PPARα* (K), and *Nfκb* (L) were evaluated. Data shown as the mean (±SE) of 5 mice per group. Statistical significance, relative to 0% vehicle control (VC), was determined by Kruskal-Wallis with Dunn's post-test (A–I) or one-way ANOVA with Dunnett's post-test (J–L) where *$p < 0.05$, **$p < 0.01$, ***$p < 0.001$. Note: The 15% PFBA exposure group received treatment on days 1–8, 14, 15, 17, 18, 22, 25, and 28 for a total of 15 days.

NK cells, eosinophils and neutrophils in the skin (Table 2) after a 28-day exposure to PFBA. Interestingly, 15% PFBA also induced an increase in both frequency and number of B-cells in the dLN (Table 1). This increase suggests the induction of an adaptive immune response and potential immunomodulatory properties for PFBA (Fairley et al., 2007). However, this increase in B-cells was not observed in the spleen (Supp. Table 5) nor was any effect on spleen % weight observed (Fig. 1C), making the biological relevance questionable. While a reduction in total spleen weight was not observed, the reduction of total cells and number of B-cells in the 7.5% group reflects similar changes as observed following dermal PFOA exposure in the spleen, although to a lesser extent (Shane et al., 2020). The biological relevance of this finding is difficult to ascertain as it was only observed in one treatment group (7.5%). A possible explanation could be due to the modification of the dosing protocol in the 15% group and the shortened half-life of PFBA.

Hepatocellular hypertrophy and an increase in liver weight is considered non-adverse/adaptive when a xenobiotic provokes only minimal to slight severity without necrosis, stimulates PPARα, and does

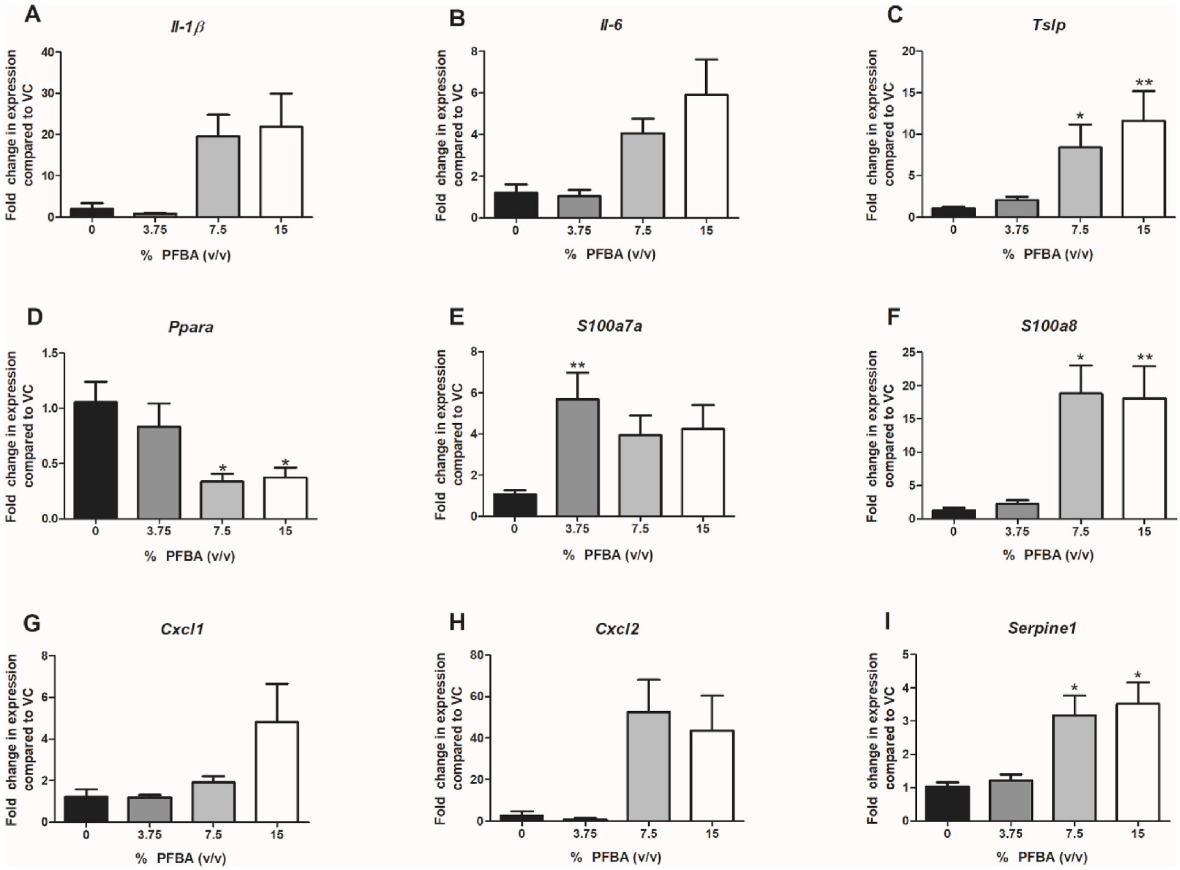

Fig. 6. Skin gene expression following dermal exposure to PFBA. Gene expression in the ear following 28 days of PFBA exposure. Changes in *Il-1β* (A), *Il-6* (B), *Tslp* (C), *Pparα* (D), *S100a7a* (E), *S100a8* (F), *Cxcl1* (G), *Cxcl2* (H), and *Serpine1* (I) were evaluated. Data shown as the mean (±SE) of 5 mice per group. Statistical significance, relative to 0% vehicle control (VC), was determined by Kruskal-Wallis with Dunn's post-test (A-C, E-I) or one-way ANOVA with Dunnett's post-test (D) where *$p < 0.05$, **$p < 0.01$. Note: The 15% PFBA exposure group received treatment on days 1–8, 14, 15, 17, 18, 22, 25, and 28 for a total of 15 days.

not induce an increase in liver enzyme activity (Hall et al., 2012). In the current study, the hepatocellular hypertrophy was classified as mild in 2/5 mice, moderate in 3/5, and mild in 5/5 mice at 3.75%, 7.5%, and 15%, respectively (Table 3). Necrosis was also present in 1/5 mice at both 3.75% and 7.5% PFBA. No necrosis was present with 15% PFBA exposure, most likely due to the intermittent dosing schedule (15 days total) with 15% PFBA (see methods section). In support of necrosis occurring, *Serpine1* expression (involved in necrosis) was increased in the liver 11- and 12-fold at 7.5% and 15%, respectively (Fig. 5C). Liver enzyme activity was also altered in the serum with an increase in ALKP and a decrease in BUN (Fig. 2). ALKP increase was also observed in male rats exposed to PFBA for 90 days, with no increase in ALT or AST (Butenhoff et al., 2012). Elevated levels of ALKP in the blood are most commonly caused by liver disease; when the liver is damaged, ALKP can leak into the blood stream. Gene expression results also support alterations in liver enzyme activity with upregulation in genes involved in phospholipidosis (*Fabp1, Hpn, Lss*) and steatosis (*Cd36, Fasn, Lpl, Scd1*) (Fig. 5; Supp. Table 6). Another study with oral PFBA exposure observed an increase in liver weight with hepatocellular hypertrophy, vacuolation, and necrosis in wildtype and humanized PPARα mice, suggesting that oral PFBA exposure has adverse liver effects (Foreman et al., 2009). These data support the suggestion that the many and interconnected effects observed in the liver meet the criteria for adversity, however, additional research is necessary. While similar results were observed in the liver for PFOA and PFBA, PFBA did not induce significant findings in the spleen in weight, phenotyping (Fig. 1C, Supp. Table 5), or histopathology (data not shown), contrary to what has been described for PFOA (Shane et al., 2020; Guo et al., 2021). The increased kidney weights with PFBA exposure (Fig. 1B) are similar to that observed with dermal PFOA exposure (Shane et al., 2020), however, this was in the absence of any remarkable histopathology (data not shown).

It is important to note that these studies were conducted for the purpose of hazard identification. Therefore, the highest non-overtly toxic concentrations were selected for evaluation following dermal exposure. Additionally, the drinking water and tail marking for animal identification are sources for potential PFAS contributions. However, these contributions are expected to be minimal and normalized relative to PFBA exposure since all groups were exposed. In conclusion, dermal exposure to PFBA generated similar results to those reported for oral PFBA and oral and dermal PFOA exposure, raising concern about the toxicity generated through the skin. Additionally, these finding demonstrate similar toxicity, qualitatively, between long chain and short chain PFAS, suggesting that long chain length may not be a valid prerequisite in the development of systemic toxicity. Understanding the hazards of skin exposure is essential for the proper implementation of protective measures to reduce risk and ensure worker safety and health.

Funding information

This work was supported by internal funds from the Health Effects Laboratory Division of the National Institute for Occupational Safety and Health.

CRediT authorship contribution statement

Lisa M. Weatherly: Conceptualization, Methodology, Formal analysis, Investigation, Writing – original draft. **Hillary L. Shane:** Conceptualization, Methodology, Formal analysis, Investigation, Writing –

review & editing. **Ewa Lukomska:** Resources. **Rachel Baur:** Writing – review & editing. **Stacey E. Anderson:** Conceptualization, Methodology, Formal analysis, Investigation, Writing – review & editing, Supervision.

Declaration of competing interest

The authors declare no conflicts of interest. The authors alone are responsible for the content of this manuscript. The findings and conclusions in this report are those of the authors and do not necessarily represent the official position of the National Institute for Occupational Safety and Health, Centers for Disease Control and Prevention. All study data will be made available on the NIOSH Data and Statistics Gateway.

Appendix A. Supplementary data

Supplementary data to this article can be found online at https://doi.org/10.1016/j.fct.2021.112528.

References

Abbott, B.D., Wolf, C.J., Schmid, J.E., Das, K.P., Zehr, R.D., Helfant, L., Nakayama, S., Lindstrom, A.B., Strynar, M.J., Lau, C., 2007. Perfluorooctanoic acid induced developmental toxicity in the mouse is dependent on expression of peroxisome proliferator activated receptor-alpha. Toxicol. Sci. 98, 571–581.

Abe, T., Takahashi, M., Kano, M., Amaike, Y., Ishii, C., Maeda, K., Kudoh, Y., Morishita, T., Hosaka, T., Sasaki, T., Kodama, S., Matsuzawa, A., Kojima, H., Yoshinari, K., 2017. Activation of nuclear receptor CAR by an environmental pollutant perfluorooctanoic acid. Arch. Toxicol. 91, 2365–2374.

ATSDR, (Agency for Toxic Substances and Disease Registry), 2018. Toxicological profile for perfluoroalkyls. Draft for public comment. Atltant, GA.

Begley, T.H., White, K., Honigfort, P., Twaroski, M.L., Neches, R., Walker, R.A., 2005. Perfluorochemicals: potential sources of and migration from food packaging. Food Addit. Contam. 22, 1023–1031.

Biegel, L.B., Hurtt, M.E., Frame, S.R., O'Connor, J.C., Cook, J.C., 2001. Mechanisms of extrahepatic tumor induction by peroxisome proliferators in male CD rats. Toxicol. Sci. 60, 44–55.

Bjork, J.A., Butenhoff, J.L., Wallace, K.B., 2011. Multiplicity of nuclear receptor activation by PFOA and PFOS in primary human and rodent hepatocytes. Toxicology 288, 8–17.

Butenhoff, J.L., Bjork, J.A., Chang, S.C., Ehresman, D.J., Parker, G.A., Das, K., Lau, C., Lieder, P.H., van Otterdijk, F.M., Wallace, K.B., 2012. Toxicological evaluation of ammonium perfluorobutyrate in rats: twenty-eight-day and ninety-day oral gavage studies. Reprod. Toxicol. 33, 513–530.

Cashman, M.W., Reutemann, P.A., Ehrlich, A., 2012. Contact dermatitis in the United States: epidemiology, economic impact, and workplace prevention. Dermatol. Clin. 30, 87–98 (viii).

Crissman, J.W., Goodman, D.G., Hildebrandt, P.K., Maronpot, R.R., Prater, D.A., Riley, J. H., Seaman, W.J., Thake, D.C., 2004. Best practices guideline: toxicologic histopathology. Toxicol. Pathol. 32, 126–131.

Das, K.P., Grey, B.E., Zehr, R.D., Wood, C.R., Butenhoff, J.L., Chang, S.C., Ehresman, D. J., Tan, Y.M., Lau, C., 2008. Effects of perfluorobutyrate exposure during pregnancy in the mouse. Toxicol. Sci. 105, 173–181.

Das, K.P., Wood, C.R., Lin, M.T., Starkov, A.A., Lau, C., Wallace, K.B., Corton, J.C., Abbott, B.D., 2017. Perfluoroalkyl acids-induced liver steatosis: effects on genes controlling lipid homeostasis. Toxicology 378, 37–52.

DeLuca, J.G., Doebber, T.W., Kelly, L.J., Kemp, R.K., Molon-Noblot, S., Sahoo, S.P., Ventre, J., Wu, M.S., Peters, J.M., Gonzalez, F.J., Moller, D.E., 2000. Evidence for peroxisome proliferator-activated receptor (PPAR)alpha-independent peroxisome proliferation: effects of PPARgamma/delta-specific agonists in PPARalpha-null mice. Mol. Pharmacol. 58, 470–476.

Du, G., Sun, J., Zhang, Y., 2018. Perfluorooctanoic acid impaired glucose homeostasis through affecting adipose AKT pathway. Cytotechnology 70, 479–487.

Fairley, K.J., Purdy, R., Kearns, S., Anderson, S.E., Meade, B., 2007. Exposure to the immunosuppressant, perfluorooctanoic acid, enhances the murine IgE and airway hyperreactivity response to ovalbumin. Toxicol. Sci. 97, 375–383.

Foreman, J.E., Chang, S.C., Ehresman, D.J., Butenhoff, J.L., Anderson, C.R., Palkar, P.S., Kang, B.H., Gonzalez, F.J., Peters, J.M., 2009. Differential hepatic effects of perfluorobutyrate mediated by mouse and human PPAR-alpha. Toxicol. Sci. 110, 204–211.

Franko, J., Meade, B.J., Frasch, H.F., Barbero, A.M., Anderson, S.E., 2012. Dermal penetration potential of perfluorooctanoic acid (PFOA) in human and mouse skin. J. Toxicol. Environ. Health 75, 50–62.

Gomis, M.I., Vestergren, R., Borg, D., Cousins, I.T., 2018. Comparing the toxic potency in vivo of long-chain perfluoroalkyl acids and fluorinated alternatives. Environ. Int. 113, 1–9.

Guo, H., Zhang, H., Sheng, N., Wang, J., Chen, J., Dai, J., 2021. Perfluorooctanoic acid (PFOA) exposure induces splenic atrophy via overactivation of macrophages in male mice. J. Hazard Mater. 407, 124862.

Hall, A.P., Elcombe, C.R., Foster, J.R., Harada, T., Kaufmann, W., Knippel, A., Küttler, K., Malarkey, D.E., Maronpot, R.R., Nishikawa, A., Nolte, T., Schulte, A., Strauss, V., York, M.J., 2012. Liver hypertrophy: a review of adaptive (adverse and non-adverse) changes–conclusions from the 3rd International ESTP Expert Workshop. Toxicol. Pathol. 40, 971–994.

Heo, J.J., Lee, J.W., Kim, S.K., Oh, J.E., 2014. Foodstuff analyses show that seafood and water are major perfluoroalkyl acids (PFAAs) sources to humans in Korea. J. Hazard Mater. 279, 402–409.

Heydebreck, F., Tang, J., Xie, Z., Ebinghaus, R., 2016. Emissions of per- and polyfluoroalkyl substances in a textile manufacturing plant in China and their relevance for workers' exposure. Environ. Sci. Technol. 50, 10386–10396.

Hui, Z., Li, R., Chen, L., 2017. The impact of exposure to environmental contaminant on hepatocellular lipid metabolism. Gene 622, 67–71.

Kato, K., Kalathil, A.A., Patel, A.M., Ye, X., Calafat, A.M., 2018. Per- and polyfluoroalkyl substances and fluorinated alternatives in urine and serum by on-line solid phase extraction-liquid chromatography-tandem mass spectrometry. Chemosphere 209, 338–345.

Kennedy Jr., G.L., Butenhoff, J.L., Olsen, G.W., O'Connor, J.C., Seacat, A.M., Perkins, R. G., Biegel, L.B., Murphy, S.R., Farrar, D.G., 2004. The toxicology of perfluorooctanoate. Crit. Rev. Toxicol. 34, 351–384.

Kotthoff, M., Müller, J., Jürling, H., Schlummer, M., Fiedler, D., 2015. Perfluoroalkyl and polyfluoroalkyl substances in consumer products. Environ. Sci. Pollut. Res. Int. 22, 14546–14559.

Kubwabo, C., Stewart, B., Zhu, J., Marro, L., 2005. Occurrence of perfluorosulfonates and other perfluorochemicals in dust from selected homes in the city of Ottawa, Canada. J. Environ. Monit. 7, 1074–1078.

Lau, C., Anitole, K., Hodes, C., Lai, D., Pfahles-Hutchens, A., Seed, J., 2007. Perfluoroalkyl acids: a review of monitoring and toxicological findings. Toxicol. Sci. 99, 366–394.

Li, Y., Fletcher, T., Mucs, D., Scott, K., Lindh, C.H., Tallving, P., Jakobsson, K., 2018. Half-lives of PFOS, PFHxS and PFOA after end of exposure to contaminated drinking water. Occup. Environ. Med. 75, 46–51.

Liu, H.S., Wen, L.L., Chu, P.L., Lin, C.Y., 2018. Association among total serum isomers of perfluorinated chemicals, glucose homeostasis, lipid profiles, serum protein and metabolic syndrome in adults: NHANES, 2013-2014. Environ. Pollut. 232, 73–79.

Mancini, A.J., Kaulback, K., Chamlin, S.L., 2008. The socioeconomic impact of atopic dermatitis in the United States: a systematic review. Pediatr. Dermatol. 25, 1–6.

MDH, (Minnesota Department of Health), 2017. PFBA and drinking water.

Meng, J., Liu, S., Zhou, Y., Wang, T., 2019. Are perfluoroalkyl substances in water and fish from drinking water source the major pathways towards human health risk? Ecotoxicol. Environ. Saf. 181, 194–201.

Nilsson, H., Kärrman, A., Westberg, H., Rotander, A., van Bavel, B., Lindström, G., 2010. A time trend study of significantly elevated perfluorocarboxylate levels in humans after using fluorinated ski wax. Environ. Sci. Technol. 44, 2150–2155.

NORA, 2019. National Occupational Research Agenda for Immune, Infectious and Dermal Disease Prevention (IID).

NTP, 2019. NTP Technical Report on the Toxicity Studies of Perfluoroalkyl Sulfonates (Perfluorobutane Sulfonic Acid, Perfluorohexane Sulfonate Potassium Salt, and Perfluorooctane Sulfonic Acid) Administered by Gavage to Sprague Dawley (Hsd: Sprague Dawley SD) Rats. National Toxicology Program, Research Triangle Park, NC. Toxicity Report 96.

Pan, Y., Zhang, H., Cui, Q., Sheng, N., Yeung, L.W.Y., Guo, Y., Sun, Y., Dai, J., 2017. First report on the occurrence and bioaccumulation of hexafluoropropylene oxide trimer acid: an emerging concern. Environ. Sci. Technol. 51, 9553–9560.

Pérez, F., Nadal, M., Navarro-Ortega, A., Fàbrega, F., Domingo, J.L., Barceló, D., Farré, M., 2013. Accumulation of perfluoroalkyl substances in human tissues. Environ. Int. 59, 354–362.

Permadi, H., Lundgren, B., Andersson, K., DePierre, J.W., 1992. Effects of perfluoro fatty acids on xenobiotic-metabolizing enzymes, enzymes which detoxify reactive forms of oxygen and lipid peroxidation in mouse liver. Biochem. Pharmacol. 44, 1183–1191.

Permadi, H., Lundgren, B., Andersson, K., Sundberg, C., DePierre, J.W., 1993. Effects of perfluoro fatty acids on peroxisome proliferation and mitochondrial size in mouse liver: dose and time factors and effect of chain length. Xenobiotica 23, 761–770.

Poynter, M.E., Daynes, R.A., 1998. Peroxisome proliferator-activated receptor alpha activation modulates cellular redox status, represses nuclear factor-kappaB signaling, and reduces inflammatory cytokine production in aging. J. Biol. Chem. 273, 32833–32841.

Rakhshandehroo, M., Knoch, B., Müller, M., Kersten, S., 2010. Peroxisome proliferator-activated receptor alpha target genes. PPAR Res. 2010.

Rebholz, S.L., Jones, T., Herrick, R.L., Xie, C., Calafat, A.M., Pinney, S.M., Woollett, L.A., 2016. Hypercholesterolemia with consumption of PFOA-laced Western diets is dependent on strain and sex of mice. Toxicol Rep 3, 46–54.

Rogue, A., Spire, C., Brun, M., Claude, N., Guillouzo, A., 2010. Gene expression changes induced by PPAR gamma agonists in animal and human liver. PPAR Res. 2010, 325183.

Rosen, M.B., Abbott, B.D., Wolf, D.C., Corton, J.C., Wood, C.R., Schmid, J.E., Das, K.P., Zehr, R.D., Blair, E.T., Lau, C., 2008. Gene profiling in the livers of wild-type and PPARalpha-null mice exposed to perfluorooctanoic acid. Toxicol. Pathol. 36, 592–607.

Rosen, M.B., Das, K.P., Rooney, J., Abbott, B., Lau, C., Corton, J.C., 2017. PPARα-independent transcriptional targets of perfluoroalkyl acids revealed by transcript profiling. Toxicology 387, 95–107.

Shane, H.L., Baur, R., Lukomska, E., Weatherly, L., Anderson, S.E., 2020. Immunotoxicity and allergenic potential induced by topical application of perfluorooctanoic acid (PFOA) in a murine model. Food Chem. Toxicol. 136, 111114.

Steenland, K., Fletcher, T., Stein, C.R., Bartell, S.M., Darrow, L., Lopez-Espinosa, M.J., Barry Ryan, P., Savitz, D.A., 2020. Review: evolution of evidence on PFOA and health following the assessments of the C8 Science Panel. Environ. Int. 145, 106125.

Sun, Mei, Arevalo, Elisa, Strynar, Mark, Lindstrom, Andrew, Richardson, Michael, Kearns, Ben, Pickett, Adam, Smith, Chris, Knappe, Detlef R.U., 2016. Legacy and emerging perfluoroalkyl substances are important drinking water contaminants in the cape fear river watershed of North Carolina. Environ. Sci. Technol. Lett. 3, 415–419.

Takacs, M.L., Abbott, B.D., 2007. Activation of mouse and human peroxisome proliferator-activated receptors (alpha, beta/delta, gamma) by perfluorooctanoic acid and perfluorooctane sulfonate. Toxicol. Sci. 95, 108–117.

Tollefson, J., 2016. Why the historic deal to expand US chemical regulation matters. Nature 534, 18–19.

Vanden Heuvel, J.P., Thompson, J.T., Frame, S.R., Gillies, P.J., 2006. Differential activation of nuclear receptors by perfluorinated fatty acid analogs and natural fatty acids: a comparison of human, mouse, and rat peroxisome proliferator-activated receptor-alpha, -beta, and -gamma, liver X receptor-beta, and retinoid X receptor-alpha. Toxicol. Sci. 92, 476–489.

Wang, Z., Cousins, I.T., Scheringer, M., Hungerbühler, K., 2013. Fluorinated alternatives to long-chain perfluoroalkyl carboxylic acids (PFCAs), perfluoroalkane sulfonic acids (PFSAs) and their potential precursors. Environ. Int. 60, 242–248.

Wang, Z., DeWitt, J.C., Higgins, C.P., Cousins, I.T., 2017. A never-ending story of per- and polyfluoroalkyl substances (PFASs)? Environ. Sci. Technol. 51, 2508–2518.

Wolf, D.C., Moore, T., Abbott, B.D., Rosen, M.B., Das, K.P., Zehr, R.D., Lindstrom, A.B., Strynar, M.J., Lau, C., 2008. Comparative hepatic effects of perfluorooctanoic acid and WY 14,643 in PPAR-alpha knockout and wild-type mice. Toxicol. Pathol. 36, 632–639.

Wright, Peter C., 2019. Interim recommendations to address groundwater contaminated with perfluorooctanoic acid and perfluorooctanesulfonate. In: United States Environmental Protection Agency. Washinton D.C.

Yan, S., Wang, J., Dai, J., 2015. Activation of sterol regulatory element-binding proteins in mice exposed to perfluorooctanoic acid for 28 days. Arch. Toxicol. 89, 1569–1578.

Zhang, X., Tanaka, N., Nakajima, T., Kamijo, Y., Gonzalez, F.J., Aoyama, T., 2006. Peroxisome proliferator-activated receptor alpha-independent peroxisome proliferation. Biochem. Biophys. Res. Commun. 346, 1307–1311.

Zhang, Y.M., Dong, X.Y., Fan, L.J., Zhang, Z.L., Wang, Q., Jiang, N., Yang, X.S., 2017. Poly- and perfluorinated compounds activate human pregnane X receptor. Toxicology 380, 23–29.

Zheng, F., Sheng, N., Zhang, H., Yan, S., Zhang, J., Wang, J., 2017. Perfluorooctanoic acid exposure disturbs glucose metabolism in mouse liver. Toxicol. Appl. Pharmacol. 335, 41–48.